Hydrodynamic perspective on memory in time-dependent density-functional theory

M. Thiele and S. Kümmel
Physikalisches Institut, Universität Bayreuth, D-95440 Bayreuth, Germany
(Received 18 December 2008; published 7 May 2009)

The adiabatic approximation of time-dependent density-functional theory is studied in the context of nonlinear excitations of two-electron singlet systems. We compare the exact time evolution of these systems to the adiabatically exact one obtained from time-dependent Kohn-Sham calculations relying on the exact ground-state exchange-correlation potential. Thus, we can show under which conditions the adiabatic approximation breaks down and memory effects become important. The hydrodynamic formulation of quantum mechanics allows us to interpret these results and relate them to dissipative effects in the Kohn-Sham system. We show how the breakdown of the adiabatic approximation can be inferred from the rate of change of the ground-state noninteracting kinetic energy.

DOI: 10.1103/PhysRevA.79.052503 PACS number(s): 31.15.ee, 31.70.Hq, 32.80.Rm

I. INTRODUCTION

Time-dependent density-functional theory (TDDFT) provides an attractive approach to treat electron dynamics in the nonlinear regime, where the solution of the many-electron time-dependent Schrödinger equation (TDSE) is not possible with the computational resources available today [1]. Important applications such as correlated electron dynamics in the presence of strong laser fields [2] crucially depend on methods like this. The benefit of TDDFT is mainly due to the fact that it is a rigorous reformulation of the quantum-mechanical many-body problem in terms of single-particle equations that can be integrated with moderate computational effort. The price to pay for this gain is the necessity to approximate the unknown but uniquely defined time-dependent exchange-correlation (xc) potential $v_{\mathrm{xc}}(\mathbf{r},t)$.

Most applications of TDDFT are based on an "adiabatic approximation" in which the exact $v_{\mathrm{xc}}(\mathbf{r},t)$ is replaced by an existing ground-state density functional. However, even if the exact ground-state xc potential is available for this procedure (adiabatically exact approximation), one would still introduce an error that will become important as soon as nonadiabatic or "memory" effects are non-negligible. The question of the breakdown of the adiabatic approximation is thus of major importance for any TDDFT application [3–9]. In practice, this problem is complicated further by the fact that the exact ground-state xc potential $v_{\mathrm{xc},0}$ is also unknown. Hence, in most situations, e.g., when using the adiabatic local density approximation (ALDA), it is difficult to tell apart the two possible sources of error: the adiabatic approximation of v_{xc} and the spatial approximation of $v_{\mathrm{xc},0}$. Finally, to be able to identify any introduced error, an exact reference solution is required.

It is exactly for these reasons that one-dimensional (1D) two-electron singlet systems provide an invaluable tool to study the validity range of any adiabatic approximation. Here, both the exact reference solution and the adiabatically exact approximation can be obtained [5,10,11]. Hence, we will focus on these systems to investigate the conditions for the breakdown of the adiabatic approximation. We find that nonadiabatic effects become important when the time-dependent density experiences rapid deformation. Based on this observation we derive a simple criterion for the breakdown of the adiabatic approximation related to the ground-state noninteracting kinetic energy. Both the observations and the criterion can be very well interpreted when one is taking a hydrodynamic point of view on the two-electron system.

The hydrodynamic formulation of quantum mechanics or quantum fluid dynamics (QFD) dates back to Madelung's reformulation of the single-particle TDSE in 1926 [12]. During the following years, further development of the theory with extensions to many-body systems has taken place mainly within condensed matter and nuclear physics (see, e.g., Refs. [13,14] and references therein). In the early 1980s QFD formulations [15] were among the immediate predecessors of TDDFT [16,17]. The latter finally provided rigorous existence and uniqueness proofs [16,18] both for TDDFT and QFD, i.e., the well-defined closure of the respective system of equations. Since then hydrodynamic concepts have proven very valuable to obtain a better understanding of collective electron dynamics (e.g., Refs. [19,20]) and even to find exact constraints on the properties of the exact xc potential (e.g., Ref. [21]). Many approaches to go beyond the adiabatic approximation mentioned earlier are based on hydrodynamical ideas, such as current density-functional theory [22,23] and TDDFT in a comoving Lagrangian reference frame [24–26]. Only recently, QFD for the general many-body problem has been cast in a very compact formulation for density and fluid velocity based on a rigorous microscopic expression of the exact stress tensor [24–26]. The latter approach has received much attention lately [27–29], providing a very intuitive way to assess many-electron phenomena. In this paper, we will argue that it is also suitable to analyze the role of memory effects and the validity regime of the adiabatic approximation in TDDFT.

It is found that the QFD formulation valid for the systems studied here is formally similar to well-known equations of classical hydrodynamics. This allows for a very intuitive explanation of the breakdown of the adiabatic approximation in TDDFT. Rapid density compression and rarefaction translate into strong gradients of the velocity field. The latter are linked to dissipative effects in the electron liquid, which are not correctly accounted for when memory effects are neglected. On the other hand, electron motion with no or slow

density deformation is properly described by the adiabatic approximation.

Our paper is organized as follows. In Sec. II we provide the basic theory for the 1D two-electron singlet system within Schrödinger quantum mechanics and TDDFT, define the adiabatic approximation, and list the required inversion concepts. We introduce the hydrodynamic point of view in Sec. III with further details provided in Appendixes A–C. In Sec. IV we present our results for the breakdown of the adiabatic approximation and its relation to dissipative effects before finally offering a summary and conclusions in Sec. V.

II. QUANTUM MECHANICS OF THE TWO-ELECTRON SYSTEM

A. Governing equations

The ground state $\psi_0(\mathbf{r}_1,\mathbf{r}_2)$ of the two-electron singlet system follows from the solution of the interacting static Schrödinger equation (SE) $H_0\psi_0=E_0\psi_0$, with the Hamilton operator

$$H_0=\sum_{j=1,2}\left(-\frac{\hbar^2}{2m}\nabla_j^2+v_{\mathrm{ext},0}(\mathbf{r}_j)\right)+V_{\mathrm{ee}}(|\mathbf{r}_1-\mathbf{r}_2|). \tag{1}$$

Here $v_{\mathrm{ext},0}(\mathbf{r}_j)$ is the external potential and the symmetric electron-electron interaction is given by $V_{\mathrm{ee}}(|\mathbf{r}_1-\mathbf{r}_2|)$. The time evolution of a general symmetric wave function $\psi(\mathbf{r}_1,\mathbf{r}_2,t)$ on the other hand is obtained from the solution of the TDSE, $i\hbar\partial_t\psi=H\psi$, governed by

$$H=\sum_{j=1,2}\left(-\frac{\hbar^2}{2m}\nabla_j^2+v_{\mathrm{ext}}(\mathbf{r}_j,t)\right)+V_{\mathrm{ee}}(|\mathbf{r}_1-\mathbf{r}_2|) \tag{2}$$

with the time-dependent external potential v_{ext}. The exact electron density, e.g., in the time-dependent case, can be obtained by

$$n(\mathbf{r},t)=2\int|\psi(\mathbf{r},\mathbf{r}',t)|^2d^3r'. \tag{3}$$

For the one-dimensional case, i.e., $\psi(z,z',t)$, the TDSE can be integrated numerically at bearable cost. To avoid the Coulomb singularity in 1D we employ the soft-core interaction $W(z)=e^2/\sqrt{z^2+1}$ for V_{ee} (always) and for the electron-nucleus interaction if we are dealing specifically with the helium atom. This approximation has been shown to reproduce the essential features of correlated electron dynamics [30–35]. It is also possible in one dimension to numerically invert the SE [11] to find $v_{\mathrm{ext},0}(z)$ for a given ground-state density $n_0(z)$. This will be useful for the reconstruction of certain quantities relevant in the context of TDDFT (see below).

The standard Kohn-Sham (KS) density-functional theory (DFT) representation of the two-electron singlet system consists of two noninteracting particles in the same spatial orbital $\varphi(\mathbf{r})$. For the ground state this orbital is the lowest eigenstate φ_0 of the stationary Kohn-Sham equation (KSE),

$$\left(-\frac{\hbar^2}{2m}\nabla^2+v_{\mathrm{s},0}(\mathbf{r})\right)\varphi_i(\mathbf{r})=\varepsilon_i\varphi_i(\mathbf{r}), \tag{4}$$

where the effective potential $v_{\mathrm{s},0}$ is a unique functional of the density $n_0(\mathbf{r})=2|\varphi_0(\mathbf{r})|^2$ by virtue of the Hohenberg-Kohn theorem [36]. Similarly the time-dependent Kohn-Sham equation (TDKSE),

$$i\hbar\partial_t\varphi(\mathbf{r},t)=\left(-\frac{\hbar^2}{2m}\nabla^2+v_{\mathrm{s}}(\mathbf{r},t)\right)\varphi(\mathbf{r},t), \tag{5}$$

governs the evolution of a general orbital $\varphi(\mathbf{r},t)$. Here the unique relation between v_{s} and $n(\mathbf{r},t)=2|\varphi(\mathbf{r},t)|^2$ is established by the Runge-Gross theorem [16]. Naturally, it is possible to calculate eigenstates of the KSE and to integrate the TDKSE. Furthermore, both equations can be inverted. This is especially straightforward for the KSE where, for any given density $n(\mathbf{r},t)$,

$$v_{\mathrm{s},0}(\mathbf{r},t)=\frac{\hbar^2}{m}\left[\frac{1}{4}\frac{\nabla^2n(\mathbf{r},t)}{n(\mathbf{r},t)}-\frac{1}{8}\left(\frac{\nabla n(\mathbf{r},t)}{n(\mathbf{r},t)}\right)^2\right]. \tag{6}$$

As this rule to construct $v_{\mathrm{s},0}$ relies only on the instantaneous density, t just takes the role of a parameter here. On the other hand the inversion of the TDKSE [37,38] works according to

$$\begin{aligned}v_{\mathrm{s}}(\mathbf{r},t)&=\frac{\hbar^2}{m}\frac{\nabla^2\varphi(\mathbf{r},t)}{2\varphi(\mathbf{r},t)}+i\hbar\frac{\dot{\varphi}(\mathbf{r},t)}{\varphi(\mathbf{r},t)}\\&=\frac{\hbar^2}{m}\left\{\frac{1}{4}\frac{\nabla^2n(\mathbf{r},t)}{n(\mathbf{r},t)}-\frac{1}{8}\left[\frac{\nabla n(\mathbf{r},t)}{n(\mathbf{r},t)}\right]^2\right\}\\&\quad-\hbar\left\{\dot{\alpha}(\mathbf{r},t)+\frac{\hbar}{2m}[\nabla\alpha(\mathbf{r},t)]^2\right\}\\&=v_{\mathrm{s},0}(\mathbf{r},t)-\hbar\left\{\dot{\alpha}(\mathbf{r},t)+\frac{\hbar}{2m}[\nabla\alpha(\mathbf{r},t)]^2\right\},\end{aligned} \tag{7}$$

i.e., it requires both density and phase information of $\varphi(\mathbf{r},t)=\sqrt{n(\mathbf{r},t)/2}e^{i\alpha(\mathbf{r},t)}$.

B. xc potential of TDDFT

The xs potential of TDDFT is related to the xc potential v_{xc} according to

$$v_{\mathrm{s}}(\mathbf{r},t)=v_{\mathrm{ext}}(\mathbf{r},t)+v_{\mathrm{h}}(\mathbf{r},t)+v_{\mathrm{xc}}(\mathbf{r},t) \tag{8}$$

or, for the ground-state situation (where t is again just a parameter),

$$v_{\mathrm{s},0}(\mathbf{r},t)=v_{\mathrm{ext},0}(\mathbf{r},t)+v_{\mathrm{h}}(\mathbf{r},t)+v_{\mathrm{xc},0}(\mathbf{r},t), \tag{9}$$

where $v_{\mathrm{h}}(\mathbf{r},t)=\int n(\mathbf{r}',t)V_{\mathrm{ee}}(|\mathbf{r}-\mathbf{r}'|)d^3r'$ is the Hartree potential, which is a local-in-time functional of the density. For the two-electron singlet system the exchange contribution to v_{xc} simplifies to $v_{\mathrm{x}}=-\frac{1}{2}v_{\mathrm{h}}$ so that in the following we will often consider v_{c} separately from $v_{\mathrm{hx}}=v_{\mathrm{h}}+v_{\mathrm{x}}=\frac{1}{2}v_{\mathrm{h}}$. When the initial state is the ground state, the xc potential at any given time t is a nonlocal functional of the exact time-dependent density n at all previous times, i.e., $v_{\mathrm{xc}}(\mathbf{r},t)=v_{\mathrm{xc}}[n(\mathbf{r}',t')](\mathbf{r},t)$ where $t'\leq t$. This dependency on the history of the density is usually referred to as "memory effects" in the xc potential [1,39].

Most TDDFT applications rely on the adiabatic approximation, which is defined by treating the time-dependent density at a fixed time $t=t_0$ as a ground-state density, i.e., $n(\mathbf{r},t_0)=n_0(\mathbf{r})$. Then, in the TDKSE $v_{\mathrm{xc}}(\mathbf{r},t_0)$ is substituted by one of the existing approximations of the ground-state xc potential. This procedure does not only lead to the loss of any memory effects but is also approximate with respect to the spatial nonlocality of the xc potential.

To treat the full spatial nonlocality exactly one needs to replace these approximations for $v_{\mathrm{xc}}(\mathbf{r},t_0)$ by the exact $v_{\mathrm{xc},0}[n_0(\mathbf{r}')](\mathbf{r})$ of ground-state DFT. This defines the adiabatically exact approximation which exclusively neglects the memory effects. Only recently it has become possible to construct this approximation for 1D two-electron systems [11]. In this approach a numerical representation of the exact and fully nonlocal $v_{\mathrm{xc},0}$ is obtained from Eq. (9) using the above-mentioned KSE- and SE-inversion schemes to calculate $v_{\mathrm{s},0}$ and $v_{\mathrm{ext},0}$ of the ground-state systems corresponding to n_0.

Thus, in the following, we can propagate the TDKSE in the adiabatically exact approximation using at every time step the $v_{\mathrm{xc},0}$ self-consistently obtained from the calculated density (AE-TDKSE scheme). The resulting observables can then be compared to their exact counterparts provided by the solution of the TDSE for the same process allowing us to assess the validity of the adiabatically exact approximations.

C. Exact properties of v_{xc}

Several properties of the exact v_{xc} have been derived over the years. One of them is the zero-force theorem [40],

$$\int n(\mathbf{r},t)\,\nabla v_{\mathrm{xc}}(\mathbf{r},t)d^3r=0, \tag{10}$$

which states that, as a consequence of Newton's third law, the net xc force exerted on the system as a whole is zero. This is automatically fulfilled for the adiabatically exact v_{xc}, which is at any time t the exact ground-state xc potential corresponding to the instantaneous density. For the two-electron singlet system studied here, the zero-force theorem holds also separately for both the Hartree-type exchange and the correlation part of v_{xc}.

Another important constraint is provided by the harmonic potential theorem (HPT) [21] for interacting electron dynamics in a parabolic potential with a time-dependent dipole perturbation, i.e., $v_{\mathrm{ext}}(\mathbf{r},t)=(k/2)r^2+\boldsymbol{E}(t)\cdot\mathbf{r}$. It can be shown that for this v_{ext} and any number of electrons N, the electron density is rigidly translated according to $n(\mathbf{r},t)=n_0(\mathbf{r}-\boldsymbol{X}(t))$. Here, $\boldsymbol{X}(t)=(1/N)\int\mathbf{r}n(\mathbf{r},t)d^3r$ is the center-of-mass coordinate obeying

$$m\ddot{\boldsymbol{X}}(t)=-k\boldsymbol{X}(t)-\boldsymbol{E}(t). \tag{11}$$

Thus, for $k/m=:\omega_0^2$ and, e.g., $\boldsymbol{E}(t)=\boldsymbol{E}_0\sin(\omega_{\mathrm{f}}t)$ and with $\boldsymbol{X}(0)=\dot{\boldsymbol{X}}(0)=0$,

$$\boldsymbol{X}(t)=\boldsymbol{E}_0\frac{1}{\omega_0^2-\omega_{\mathrm{f}}^2}\left(\frac{\omega_{\mathrm{f}}}{\omega_0}\sin(\omega_0t)-\sin(\omega_{\mathrm{f}}t)\right). \tag{12}$$

For TDDFT to satisfy the HPT, the xc potential needs to rigidly follow the rigidly translated density, a feature also termed generalized translational invariance [40]. When the initial state of the system is the ground state, this means that $v_{\mathrm{xc},0}$ is rigidly translated with the density, i.e., the adiabatically exact v_{xc} is valid exactly for HPT motion. Later on, when we want to establish a criterion for the validity regime of the adiabatic approximation, the fact that HPT motion always should fulfill this criterion will be of importance.

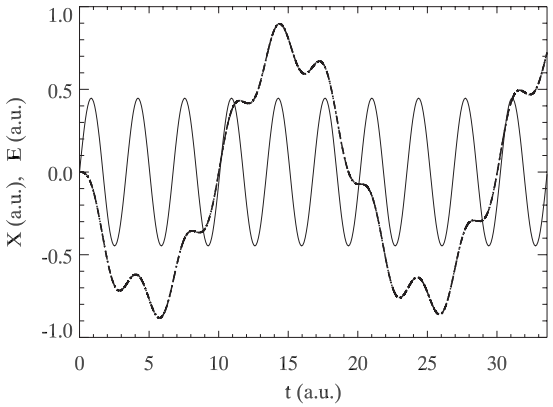

FIG. 1. Time evolution of $X(t)$ for the 1D two-electron Hooke's atom with $v_{\mathrm{ext}}(z)=(k/2)z^2+E_0z\sin(\omega_{\mathrm{f}}t)$, where $k=0.1$ a.u., $E_0=0.447$ a.u., and $\omega_{\mathrm{f}}=1.870$ a.u. The TDSE (dashed) and AE-TDKSE (dotted-dashed) curves both lie on top of the dotted one given by Eq. (12). For comparison, we also show $E(t)=E_0\sin(\omega_{\mathrm{f}}t)$ (thin solid line).

To shortly illustrate the important concept of HPT motion and to test the accuracy of the numerical realization of the AE-TDKSE scheme, we have performed calculations for a 1D Hooke's atom. We show in Fig. 1 how theory [Eq. (12)] and numerical results both from the exact TDSE and the AE-TDKSE schemes provide exactly the same evolution of $X(t)$. This shows that the AE-TDKSE scheme, which by definition should be able to reproduce HPT motion, is working very accurately. It should also be noted that the HPT theorem is valid not only in the linear regime but also for strong perturbation amplitudes E_0, as used in the test calculation on which Fig. 1 is based.

In the following, we will consider three different 1D bound systems: the "anharmonic Hooke's atom" characterized by $v_{\mathrm{ext},0}(z)=(k/2)(z^2+\tilde{k}z^6)$ (A6-Hooke) or $v_{\mathrm{ext},0}(z)=(k/2)(z^2+\tilde{k}z^4)$ (A4-Hooke) with $k=0.1$ a.u. and $\tilde{k}=0.01$ a.u. [41] (we use Hartree atomic units unless stated otherwise). The anharmonic term has been introduced to deliberately avoid HPT motion when the dipole field $ezE(t)$ is applied [5]. The third system studied is the soft-core helium atom [11,30,34,35] characterized by the ground-state potential $v_{\mathrm{ext},0}(z)=-2W(z)$. The different systems are summarized in Table I. The initial state for any time-dependent process is the ground state of the particular system.

III. HYDRODYNAMICS OF THE TWO-ELECTRON SYSTEM

After the inspection of the relevant equations of quantum mechanics we will now turn to their hydrodynamic formulation. For our purposes it will suffice to deal with the nonin-

TABLE I. Ground state properties of 1D two-electron singlet systems studied in this paper. The ground-state noninteracting kinetic energy $T_{s,0}$ is defined in Eq. (23). The lowest KS excitation frequency $\omega_{s,1}$ is determined from the 1D version of Eq. (4). The breakdown threshold $\dot{T}_{s,0}^{crit}$ is defined in Eq. (25). All values are in Hartree atomic units.

System	$v_{ext,gs}(z)$	$\omega_{s,1}$	$T_{s,0}(0)$	$\dot{T}_{s,0}^{crit}$
A6-Hooke	$k/2(z^2+\tilde{k}z^6)$ [a]	0.267	0.156	0.007
A4-Hooke	$k/2(z^2+\tilde{k}z^4)$ [a]	0.192	0.108	0.003
Helium	$-2W(z)$	0.479	0.277	0.021

[a] $k=0.1$, $\tilde{k}=0.01$.

teracting TDKSE system, which for the exact v_{xc} produces the same density as the interacting TDSE system. The QFD formulation of the TDKSE presented in the following allows for a more intuitive interpretation of the adiabatic approximation guided by well-known concepts of classical fluid dynamics. A short review of the classical theory is provided in Appendix A.

A. Governing equations

As mentioned before, the single-particle KS wave function $\varphi(\mathbf{r},t)=\sqrt{n(\mathbf{r},t)/2}e^{i\alpha(\mathbf{r},t)}$ is completely determined by the density n and the phase α. This means that we can transform the KSE system into a set of hydrodynamic equations for the density n and the KS velocity field,

$$\boldsymbol{u}_s(\mathbf{r},t)=\boldsymbol{j}_s(\boldsymbol{r},t)/n(\boldsymbol{r},t)=\frac{\hbar}{m}\boldsymbol{\nabla}\,\alpha(\boldsymbol{r},t), \tag{13}$$

where $\boldsymbol{j}_s$ is the KS current [42] by noting that $\boldsymbol{u}_s$ contains the same information as α. The transformation closely follows the one given by Madelung for the single-particle Schrödinger equation [12,43]. The details are provided in Appendix B. Finally, one arrives at the hydrodynamic set of equations consisting of the continuity equation

$$D_t n=-n\,\boldsymbol{\nabla}\cdot\boldsymbol{u}_s, \tag{14}$$

the momentum equation

$$mD_t u_{sj}=-\frac{1}{n}\partial_i(P_{sij}+\delta_{ij}p_c)-\partial_j(v_{hx}+v_{ext}) \tag{15}$$

(we use the Einstein convention of implicit sums $\Sigma_{i=1}^{3}$ over products with the same index i), and the Poisson equation

$$\Delta v_{hx}=-2\pi e^2 n. \tag{16}$$

Here $D_t=\partial_t+\boldsymbol{u}_s\cdot\boldsymbol{\nabla}$ is the convective derivative and

$$P_{sij}=\frac{\hbar^2}{4m}\left(\frac{(\partial_i n)(\partial_j n)}{n}-\delta_{ij}\nabla^2 n\right) \tag{17}$$

is the noninteracting stress tensor [24–26]. The correlation contribution p_c is defined by $\boldsymbol{\nabla}p_c=n\boldsymbol{\nabla}v_c$. The formal closure of the hydrodynamic set of equations is proven by the Runge-Gross theorem [16], which implies that p_c exists and is uniquely defined by the density n, i.e., we have an unknown but well-defined constitutive relation $p_c[n]$.

The equations for the two-electron singlet system closely resemble those derived by Madelung [12] for the single particle. Also P_{sij} has the same form as the quantum stress tensor of single-particle QFD [14,28]. This is a consequence of the singlet property of the system leading to two spatially identical KS orbitals. The only differences are due to the appearance of the correlation contribution p_c and the Hartree-exchange potential v_{hx}.

For the 1D situation that we study, where u_s denotes the z coordinate of the KS velocity, one arrives at

$$D_t n=-n\partial_z u_s \tag{18}$$

and

$$mD_t u_s=-\frac{1}{n}\partial_z p-\partial_z(v_{hx}+v_{ext}), \tag{19}$$

where $D_t=\partial_t+u_s\partial_z$. Now, $v_{hx}(z,t)=1/2\int n(z',t)W(|z-z'|)dz'$ and the tensor in Eq. (15) has collapsed into a generalized scalar pressure

$$p=p_{s,0}+p_c \tag{20}$$

with the noninteracting pressure [29]

$$p_{s,0}=\frac{\hbar^2}{4m}\left(\frac{(\partial_z n)^2}{n}-\partial_z^2 n\right). \tag{21}$$

Note that $\partial_z p_{s,0}=-n\partial_z v_{s,0}$.

At this point it is instructive to pause for a moment and have a look at the derived three-dimensional (3D) and 1D QFD equations. They are exact reformulations of the TDKSE, i.e., when the exact v_c is available, they will have the exact time-dependent density as solution. The latter is of course also provided by the QFD equations for the interacting system, which can be derived from the TDSE [24–26]. However, the exact KS velocity $\boldsymbol{u}_s$ and the exact interacting velocity $\boldsymbol{u}$ do not necessarily agree in three dimensions. This is a consequence of the open question whether KS and interacting current are identical [42]. Of course in one dimension the relation $u_s=u$ holds, allowing us for the time-dependent process at hand to identify u from the TDSE with the exact u_s. The latter can then be compared with the adiabatically exact u_s stemming from the corresponding AE-TDKSE calculation.

B. Contributions to the generalized pressure

Looking at Eqs. (18) and (19) we notice a strong structural similarity to the 1D versions of the classical hydrodynamic equations reviewed in Appendix A. To push the analogy even further we recall that the classical stress tensor (Appendix A) contains a (hydro)static density-dependent pressure part and a dynamic velocity-dependent viscous contribution. As we will show in the following, the same classification holds for the generalized pressure of Eq. (20).

We start by splitting up the correlation pressure according to $p_c=p_{c,0}+p_{c,mem}$, where the former part stems from the adiabatically exact $v_{c,0}$ while the latter includes all the

TABLE II. Time-dependent processes of the A6-Hooke and A4-Hooke systems as given in Table I with $v_{ext}(z,t)=v_{ext,gs}(z)+ezE_0\sin(\omega_f t)$. Intensity I in W/cm^2; E_0 and ω_f in Hartree atomic units. The memory character of a process follows from the deviation of the TDSE- and AE-TDKSE-solutions in time (see text).

Process	I	E_0	ω_f	Memory
A6-Hooke I	7×10^{14}	0.141	0.029	No
A6-Hooke II	7×10^{15}	0.447	1.870	Yes
A4-Hooke I	7×10^{14}	0.141	0.029	No
A4-Hooke II	7×10^{15}	0.447	1.870	Yes
A4-Hooke III	7×10^{15}	0.447	0.935	Yes

memory effects with respect to n. While $p_{s,0}$ and $p_{c,0}$ exclusively depend on the instantaneous density (nonlocal in space and local in time), the situation for $p_{c,mem}$ requires a closer inspection.

Due to the relation between KS velocity and density as provided by Eq. (14) the nonlocal-in-time relation to the density in $p_{c,mem}[n]$ can be re-expressed in terms of a dependency on the initial state density n_{gs} and on the history of the KS velocity u_s. This follows from a "kinematic" solution of Eq. (14), where from a prescribed velocity field $u_s(z,t')$ for $0\le t'\le t$ one can always reconstruct $\dot{n}(z,t')$ on the same interval. Together with $n_{gs}(z)$ this fixes $n(z,t')$ and hence $p_{c,mem}$ for $0\le t'\le t$. As a consequence $p_{c,mem}[n]$ is replaced by $\hat{p}_{c,mem}[n_{gs},u_s]$, which is a functional of n_{gs} (nonlocal in space) and velocity u_s (nonlocal in space and time).

The HPT motion mentioned earlier has a very intuitive form in the hydrodynamic picture: rigid motion of the density corresponds to purely advective motion without deformation, i.e., a continuity equation with vanishing right-hand side (rhs) or $\partial_z u_s=0$ (see Appendix A). Thus, the velocity is constant in space following $u_s=\dot{X}(t)$. In the momentum equation the nonlinear term of the convective derivative disappears and the xc pressure is replaced by its adiabatically exact contribution. This means that $\hat{p}_{c,mem}[n_{gs},u_s]=0$ here, telling us that $\hat{p}_{c,mem}$ is in fact a functional of $\partial_z u_s$, i.e., we actually have $\tilde{p}_{c,mem}[n_{gs},\partial_z u_s]$. The latter observation is a consequence of the Galilean invariance of the stress tensor [23,44], of which p is the scalar "leftover" in one dimension.

Thus $p_{s,0}$ and $p_{c,0}$ clearly provide the ground-state contribution or hydrostatic pressure [29] in Eq. (20) (recall also that $\partial_z p_{s,0}=-n\partial_z v_{s,0}$), while the dynamical component can only stem from $\tilde{p}_{c,mem}$.

IV. BREAKDOWN OF THE ADIABATIC APPROXIMATION

It has already been shown that for certain time-dependent processes, the exact and adiabatically exact xc potentials corresponding to a given exact density will be different [11]. To demonstrate that these memory effects have an observable influence on the dynamics, we have performed self-consistent AE-TDKSE calculations for several processes with and without nonadiabatic effects. The obtained results can then be compared with the exact TDSE solution. We concentrate on the anharmonic Hooke system (cf. Table II),

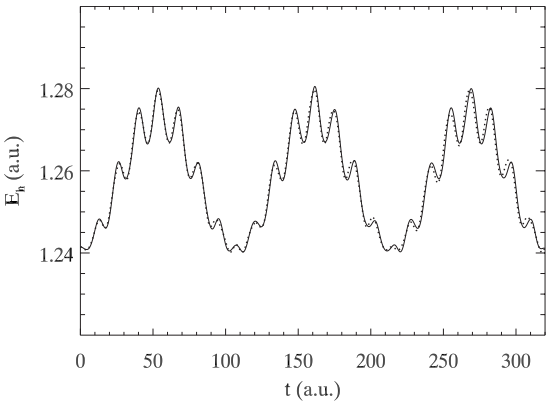

FIG. 2. Time evolution of E_h for A6-Hooke I system calculated with TDSE (solid line) and AE-TDKSE (dotted line).

which is especially suitable to analyze deviations from HPT motion while still profiting from the localization of the density due to the strong confinement provided by the parabolic potential.

A. A6-Hooke process without memory

We start with the A6-Hooke I process, for which the driving field intensity and frequency are in the range of typical strong laser processes (cf. Table II). Figures 2 and 3 show the evolution of the Hartree energy $E_h(t)=1/2\int n(z,t)v_h(z,t)dz$ and of the ground-state noninteracting kinetic energy $T_{s,0}(t)$ for both the TDSE and AE-TDKSE calculations. We choose these observables for monitoring memory because of their direct scalar dependence on the density [5]. $T_{s,0}(t)$ is defined as

$$T_{s,0}(t)=\frac{\hbar^2}{m}\int[\partial_z\varphi_0(z,t)]^2dz, \tag{22}$$

where $\varphi_0(z,t)=\sqrt{n(z,t)/2}$ and thus,

$$T_{s,0}(t)=\frac{\hbar^2}{8m}\int\frac{[\partial_z n(z,t)]^2}{n(z,t)}dz, \tag{23}$$

with similar relations for the 3D case. The good agreement of the TDSE and AE-TDKSE results indicates that the adia-

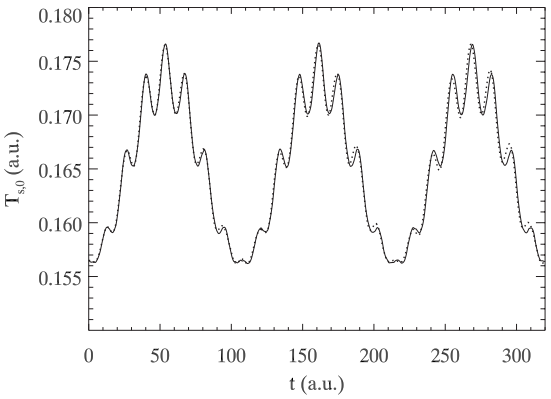

FIG. 3. Time evolution of $T_{s,0}$ for A6-Hooke I system calculated with TDSE (solid line) and AE-TDKSE (dotted line).

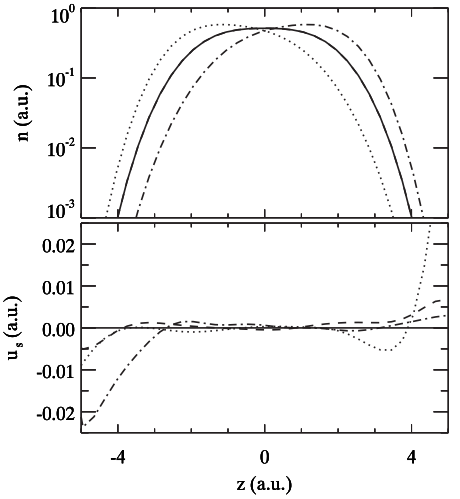

FIG. 4. Snapshots of exact density n and velocity u_s during A6-Hooke I process. According to Eq. (13) the velocity increases as the density drops (e.g., around $z=4$ a.u.). The resulting velocity gradients in regions of very low density are discussed further below.

batically exact approximation is valid here. Figure 4 shows snapshots of typical densities and velocities during this process. Although there is not only bulk motion but also some density deformation going on, it apparently happens on a slow enough time scale for the adiabatic approximation to remain valid. The slowness of the density deformation corresponds to almost flat velocity profiles according to Eq. (18), indicating that the instantaneous velocity is a more suitable quantity in this context than the instantaneous density deformation. Note that in the 1D situation studied in this paper density deformation always corresponds to density compression on the one hand and rarefaction on the other as at least two dimensions are required for a finite fluid volume to deform its shape while conserving its volume.

B. A6-Hooke process with memory

Now we turn our attention to a process at higher intensity and frequency (A6-Hooke II process) and repeat the analysis with respect to the energies. Figures 5 and 6 show the evolution of E_h and $T_{s,0}$ for both the TDSE and AE-TDKSE calculations. In striking contrast to the situation before, we can see that around $t \approx 3.5$ a.u. the solutions start to differ.

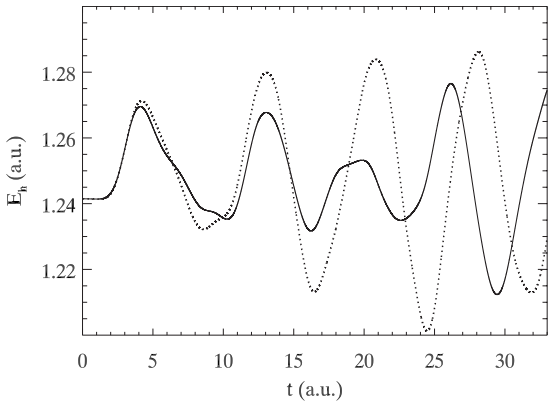

FIG. 5. Time evolution of E_h for A6-Hooke II system calculated with TDSE (solid line) and AE-TDKSE (dotted line).

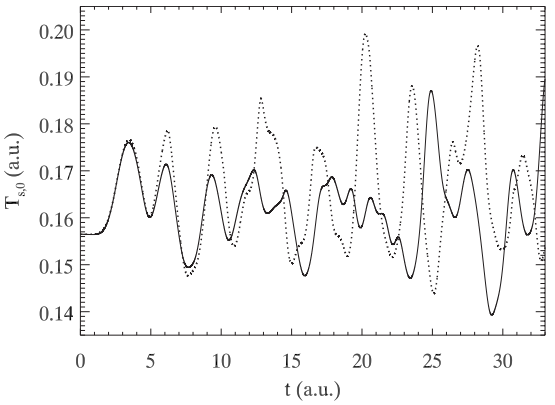

FIG. 6. Time evolution of $T_{s,0}$ for A6-Hooke II system calculated with TDSE (solid line) and AE-TDKSE (dotted line).

The different density evolutions in the two calculations indicate the insufficiency of the adiabatic approximation for this process. To analyze the conditions of the breakdown, it is instructive to compare the evolution of the density and velocity field for TDSE and AE-TDKSE calculations during the time interval where the energies start to deviate (Figs. 7–9). As in the A6-Hooke I process, the density gets deformed compared to HPT motion. But now this deformation is happening more rapidly, i.e., strong gradients appear in the velocity. This is a situation that is completely unlike the HPT motion described earlier as it leads to regions of either rapid density compression or rarefaction. Such behavior has been discussed in several earlier works: strong velocity gradients were shown to lead to the breakdown of the approximation of Vignale, Ullrich, and Conti [23] for the description of collective intersubband transitions in quantum wells [45] and of $s \rightarrow p$ transitions in atomic systems [46]. Similarly, it has been observed that rapid and strong density deformation

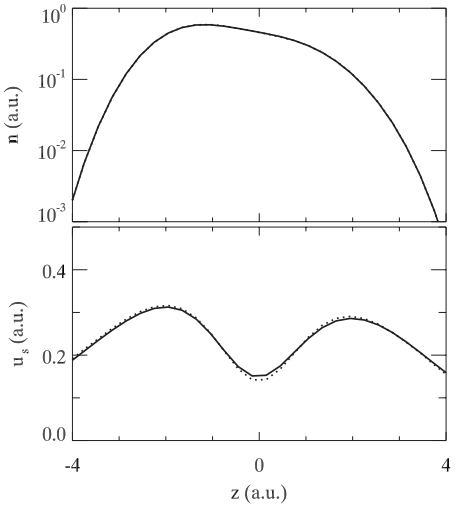

FIG. 7. Comparison of densities and velocities from TDSE (solid line) and AE-TDKSE (dotted line) schemes at $t=3.36$ a.u. for A6-Hooke II system.

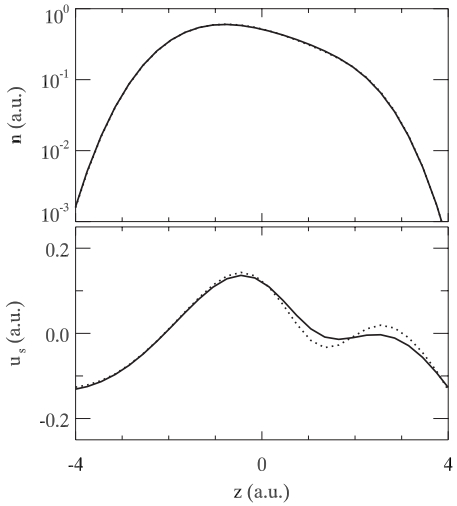

FIG. 8. Comparison of densities and velocities from TDSE (solid line) and AE-TDKSE (dotted line) schemes at $t=4.20$ a.u. for A6-Hooke II system.

leads to failure of the ALDA [7] and the time-dependent Krieger-Li-Iafrate approximations [9] in simple model systems. However, all these approaches are approximate not only in their nonlocal-in-time dependency on the density but also with respect to nonlocality in space. The adiabatically exact approximation which we use here allows us to investigate the exclusive relation between strong density deformation and memory effects while treating the nonlocality in space exactly.

The appearance of strong gradients in the velocity field has been related to a transition of the system from mostly collective toward single-particle-like motion [7,45]. However, for the two-electron singlet case this concept has to be refined as the motion here is always collective in the sense that only two equivalent orbitals exist and evolve exactly in the same way. Hence the velocity gradients cannot arise from differences in the single-particle currents, which were identified to be a reason for noncollective motion in systems with more electrons [47]. So, for the two-electron singlet system, it might be more appropriate to regard velocity gradients as a deviation from rigid "bulk motion" of the density distribution.

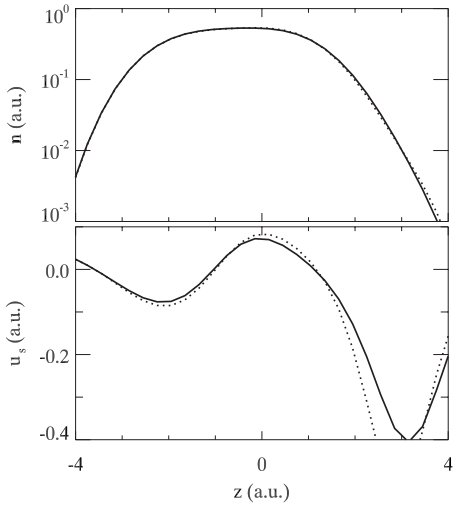

FIG. 9. Comparison of densities and velocities from TDSE (solid line) and AE-TDKSE (dotted line) schemes at $t=5.46$ a.u. for A6-Hooke II system.

So why and how are strong velocity gradients related to the breakdown of the adiabatic approximation? It is instructive to now look back at the essential features of the hydrodynamic equations derived above. In the adiabatic approximation, where $\tilde{p}_{\mathrm{c,mem}}[n_{\mathrm{gs}},\partial_z u_{\mathrm{s}}]=0$, we are dealing with a momentum equation that strongly resembles the Euler equation, i.e., no velocity-dependent components appear on the rhs as would be the case for, e. g., the Navier-Stokes equation. Thus, it is immediately clear that as soon as strong velocity gradients develop, the nonlinear term $u_{\mathrm{s}}\partial_z u_{\mathrm{s}}$ on the left-hand side will become dominant for the time evolution because there is no term $\tilde{p}_{\mathrm{c,mem}}[n_{\mathrm{gs}},\partial_z u_{\mathrm{s}}]$ on the rhs, which could balance it. Hence, one should indeed expect that the solutions of calculations with and without $\tilde{p}_{\mathrm{c,mem}}[n_{\mathrm{gs}},\partial_z u_{\mathrm{s}}]$ start to deviate in such a situation.

From the analogy of $\tilde{p}_{\mathrm{c,mem}}[n_{\mathrm{gs}},\partial_z u_{\mathrm{s}}]$ to the viscous stress contributions in classical hydrodynamics it follows that its reaction to strong velocity gradients is, at least to leading order, of dissipative nature. Here, the term dissipation specifically refers to the dissipation of classical (collective) kinetic energy through a diffusive term in the momentum equation, i.e., the nonadiabatic term, $\tilde{p}_{\mathrm{c,mem}}$, can lead to dissipation of the velocity field's kinetic energy. The latter does not disappear from the system but can be transferred to other internal energy components. It should be mentioned that further contributions to $\tilde{p}_{\mathrm{c,mem}}[n_{\mathrm{gs}},\partial_z u_{\mathrm{s}}]$ may also lead to energy injection. Nonadiabatic effects of velocity-dependent contributions have also been shown to be connected to entropy production and irreversible relaxation in infinite systems [48].

Generally, there seems to be a tendency of the AE-TDKSE solution to lead to more pronounced gradients than the TDSE (cf. Figs. 8 and 9). This appears quite reasonable, as it is well known that due to the nonlinear convective term $u_{\mathrm{s}}\partial_z u_{\mathrm{s}}$, the 1D Euler equation can build up discontinuities in the velocity field [49]. This effect can be balanced by a dissipative velocity-dependent term on the rhs, as frequently studied in one dimension in the context of the viscous Burger's equation [49]. However, due to the nature of the adiabatic approximation, any velocity-dependent term on the rhs of Eq. (19) is excluded. Thus, a "smoothing" or damping effect on the buildup of velocity gradients is not available in this situation. The absence of such a mechanism does generally not pose a problem for a quantum system, as discontinuities in the (not observable) velocity just signal kinks in the phase [cf. Eq. (13)]. But here, it will clearly make the phase of the adiabatically exact system start to differ from that of the exact system, leading to a different time evolution of the whole process and thus to the breakdown of the adiabatic approximation.

We have seen that the development of strong gradients in the velocity will threaten the validity of the adiabatic approximation. One should also note that the main effect of this feature on the observable quantity of interest, namely, the density n, is due to the rhs of the continuity equation [Eq.

(18)]. This indicates that the effect is weighted by the density $(n\partial_z u_s)$, showing that the strong gradients might be less important in regions where the density is small. Note that in the limit of vanishing density the definition of the velocity breaks down anyway [28]. In a way, one could also regard those parts of the flow where the rhs of Eq. (18) vanishes due to vanishing n and/or $\partial_z u_s$ as approximately incompressible and hence not problematic for the adiabatic approximation. In these regions the density is just advected by the velocity field as a whole without any deformation happening (cf. Appendix A). An important limiting case is of course electron motion according to the harmonic potential theorem, where $\partial_z u_s$ vanishes exactly and, as stated above, the adiabatic approximation is exactly valid.

C. Breakdown criterion

While the obtained results and the hydrodynamic argument provide us with a good qualitative understanding of the adiabatic approximation, the appearance of strong velocity gradients does not offer a very practical criterion to determine when its breakdown will actually occur. Ideally one would like to infer already from the type, frequency, and strength of the applied perturbation whether an adiabatic approach is justified. However, facing the whole scope of possible strong field excitations, it seems too ambitious to predict the appearance of strong density gradients just from looking at $v_{\mathrm{ext}}(z,t)$. Instead, we will in the following present a simple criterion that will tell us, for an ongoing time-dependent KS calculation, when the adiabatic approximation is most certainly breaking down and the density evolution will start to differ from the exact one.

A suitable criterion that is based on the density should be sensitive to its rapid deformation, which, as shown above, corresponds to strong velocity gradients in regions of finite n. To this end, we turn back to $T_{s,0}$, which basically provides an integral measure of the curvature and hence the deformation of the instantaneous density. As we are not interested in the absolute deformation of the density but rather how rapidly it changes in time, it is advantageous to look at

$$\begin{aligned}\dot{T}_{s,0} &= -\int j_s \partial_z v_{s,0} dz \\ &= -\int n u_s \partial_z v_{s,0} dz \\ &= \int u_s \partial_z p_{s,0} dz \\ &= -\int p_{s,0} \partial_z u_s dz. \end{aligned} \tag{24}$$

There are several additional reasons why this quantity might be suitable for a memory criterion: it has been shown [5] that time derivatives of energy components can indicate memory effects. Additionally, $\dot{T}_{s,0}$ is based on just the orbitals, i.e., it is always available in any time-dependent KS scheme. Furthermore, we see that $\dot{T}_{s,0}$ provides an integral measure of the velocity gradient $\partial_z u_s$ weighted with the noninteracting pressure $p_{s,0}$. The latter quantity vanishes in regions where the density falls off to zero and hence ensures that velocity gradients in regions of low density will contribute less to $\dot{T}_{s,0}$. Finally, $T_{s,0}$ can be regarded as a quantity intimately related to the ground-state character of a given density. The latter is expected to change rapidly in any nonadiabatic process.

Another attractive feature of $\dot{T}_{s,0}$ is that in the limit of HPT motion without deformation, $\dot{T}_{s,0}$ vanishes exactly as $\partial_z u_s = 0$ in Eq. (24). Note that this property is shared by, e.g., $\dot{E}_h$, but the latter is much more sensitive to the density distribution in space than to its deformation.

In the following we will define an approximate upper bound for $|\dot{T}_{s,0}(t)|$ of an ongoing time-dependent process that is still adiabatic. This bound is provided by the ratio

$$\dot{T}_{s,0}^{\mathrm{crit}} = \frac{T_{s,0}(t=0)}{\tau^{\mathrm{mem}}}, \tag{25}$$

where $T_{s,0}(t=0)$ is the initial value of the ground-state noninteracting kinetic energy of the system under study. τ^{mem} is the memory time scale defined in the following way: as soon as a process is happening on the time scale τ^{mem} (or on shorter time scales), it is expected to be no longer adiabatic. To fix τ^{mem} we consider the limit of the linear response of the system. Here memory is known to become important as soon as the considered process takes place at a frequency ω at which the xc kernel, $\delta v_{\mathrm{xc}}[n]/\delta n$, shows significant frequency dependence [1,4]. As the xc kernel is composed of the inverse response functions of the interacting and the noninteracting systems, it will "inherit" their frequency dependence. This means that a good estimate for an upper bound for the frequency range where the xc kernel is almost independent of ω is provided by the lowest occurring transition frequency [50]. For the systems studied here this is the lowest KS transition energy $\omega_{s,1} = (\varepsilon_1 - \varepsilon_0)/\hbar$ (cf. Table I). Thus it makes sense to define $\tau^{\mathrm{mem}} = 2\pi/\omega_{s,1}$. Consequently an approximate upper bound for the validity of the adiabatic approximation for a specific process is provided by $|\dot{T}_{s,0}(t)| < \dot{T}_{s,0}^{\mathrm{crit}}$. The possibility to extend this criterion to the case of more than two electrons in three dimensions is discussed in Appendix C.

Figure 10 shows the exact evolution of $\dot{T}_{s,0}(t)$ for the two A6-Hooke systems together with the upper bound for $|\dot{T}_{s,0}(t)|$ according to Eq. (25). $\dot{T}_{s,0}(t)$ differs strongly for both processes and the proposed criterion clearly separates both regimes.

Figure 11 shows $\dot{T}_{s,0}(t)$ for a larger data set of TDSE calculations for the A6-Hooke system (cf. Table III), where the memory character of each process has been determined by comparing v_c and $v_{c,0}$ obtained from the inversion schemes. Although the applied dipole fields vary strongly with respect to E_0 and ω_f, the criterion seems to hold in a large part of the parameter space. Note that the procedure used here to determine memory effects is not completely equivalent to the approach presented before. Therefore, the data shown in Fig. 11 should be seen more as a trend for the applicability of the adiabatic approximation with respect to the parameters E_0 and ω_f for a given system. These results

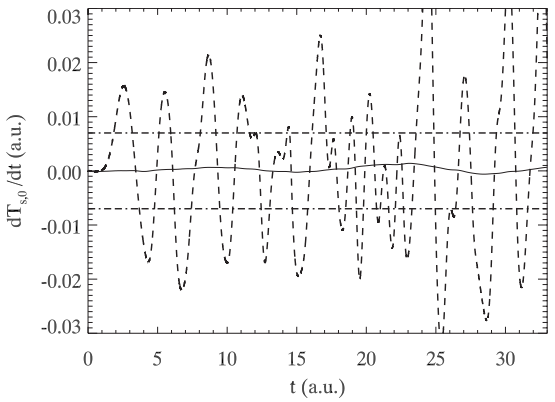

FIG. 10. Exact evolution of $\dot{T}_{s,0}$ for A6-Hooke systems I (without memory, solid line) and II (with memory, dashed line). The dotted-dashed line represents the memory criterion according to Table I and formula (25).

also indicate that $\dot{T}_{s,0}^{crit}$ provides an upper bound for (and not the maximum of) the $|\dot{T}_{s,0}(t)|$ that can occur during a still adiabatic process. On the other hand with $|\dot{T}_{s,0}| \geq \dot{T}_{s,0}^{crit}$ the adiabatic approximation is certainly breaking down.

To show the applicability of the criterion to different systems we consider the A4-Hooke I–III processes. Figure 12 shows the exact evolution of $\dot{T}_{s,0}(t)$ for the three processes together with the appropriate criterion. Here again, $|\dot{T}_{s,0}(t)| > \dot{T}_{s,0}^{crit}$ correctly indicates memory effects for A4-Hooke III process. The regime $|\dot{T}_{s,0}(t)| < \dot{T}_{s,0}^{crit}$ covers both the adiabatic A4-Hooke I process at almost vanishing $|\dot{T}_{s,0}|$ and the nonadiabatic A4-Hooke II process with relatively high $|\dot{T}_{s,0}|$. These findings highlight once more that $\dot{T}_{s,0}^{crit}$ has the character of an approximate upper bound for the adiabatic regime.

For completeness we also show in Fig. 13 three different processes in the helium atom studied previously [11]. Although the helium system differs qualitatively from the anharmonic Hooke case and the studied processes are of different types the criterion works similarly well here.

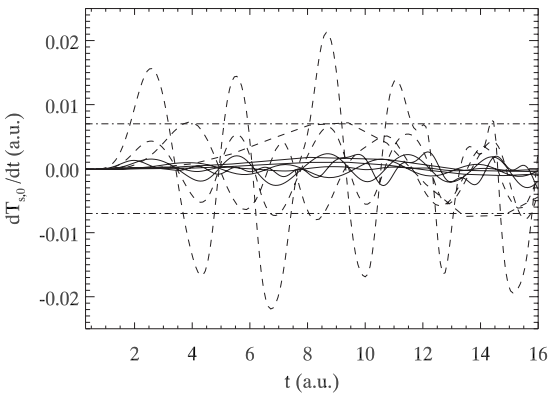

FIG. 11. Exact evolution of $\dot{T}_{s,0}$ for A6-Hooke processes described in Table III (without memory: solid lines; with memory: dashed line). The dotted-dashed line represents the memory criterion according to Table I and formula (25).

TABLE III. Time-dependent processes of A6-Hooke in a dipole field according to $v_{ext}(z,t) = v_{ext,gs}(z) + ezE_0 \sin(\omega_f t)$. Intensity I in W/cm^2; E_0 and ω_f in Hartree atomic units. The memory character of a process follows from the deviation of v_c and $v_{c,0}$ corresponding to the exact time-dependent density.

I	E_0	ω_f	Memory
1×10^{14}	0.053	0.117	No
1×10^{14}	0.053	0.935	No
7×10^{14}	0.141	0.058	No
7×10^{14}	0.141	0.117	Yes
7×10^{14}	0.141	0.935	Yes
7×10^{14}	0.141	1.870	No
1×10^{15}	0.169	3.740	No
2×10^{15}	0.239	1.870	Yes
2×10^{15}	0.239	2.805	No
7×10^{15}	0.447	1.870	Yes

V. CONCLUSION

We have studied the conditions for the breakdown of the adiabatic approximation in TDDFT. To allow for a numerically exact analysis of this problem we focused on 1D two-electron singlet systems where both exact and adiabatically exact calculations are possible. To interpret the results and proceed toward a quantitative criterion for the breakdown, we have transformed the governing equations into a hydrodynamic formulation based on the density n and the KS velocity u_s.

The breakdown of the adiabatic approximation was found to be related to the appearance of strong velocity gradients corresponding to rapid compression and rarefaction of the density. Within the hydrodynamic picture these features can be clearly linked to dissipative effects in the KS system that are missed whenever the adiabatic approximation is used. Guided by this observation we derived a criterion for the breakdown of the adiabatic approximation based on the rate of change of the ground-state noninteracting kinetic energy.

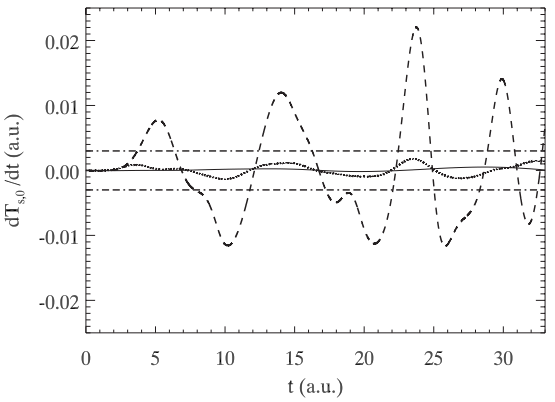

FIG. 12. Exact evolution of $\dot{T}_{s,0}$ for A4-Hooke systems I (without memory, solid line), II (with memory, dotted line), and III (with memory, dashed line). The dotted-dashed line represents the memory criterion according to Table I and formula (25).

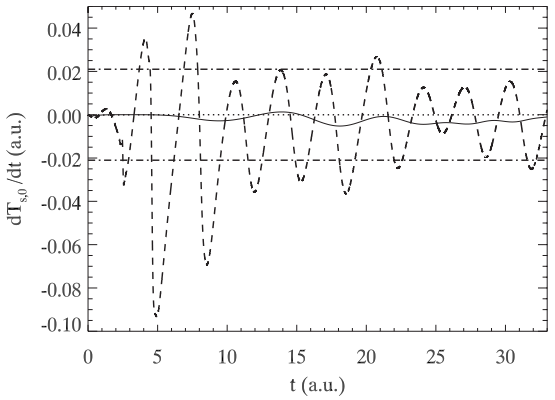

FIG. 13. Exact evolution of $\dot{T}_{s,0}$ for helium systems ramp (without memory, solid line), pulse with $I=7\times10^{14}$ W/cm^2 (without memory, dotted line), and oscillating nucleus (with memory, dashed line) as investigated in Ref. [11]. The dotted-dashed line represents the memory criterion according to Table I and formula (25). For the pulse $\dot{T}_{s,0}$ is reaching finite amplitudes at later times but not exceeding 40% of $\dot{T}_{s,0}^{crit}$.

The latter provides an integral measure of strong velocity gradients in regions of finite density. We showed that this criterion provides an approximate upper bound for the validity of the adiabatic approximation for a given time-dependent process.

The evaluation of the criterion for different processes indicates that memory effects generally become more important for growing strength of the external perturbation. However, for forcing frequencies that are very low the adiabatic approximation is found to hold even at strong perturbation amplitudes. In the opposite limit of very high frequencies there are also indications for the applicability of the adiabatic approximation in agreement with recent analytical findings [51]. This behavior agrees with the analogy between the electron liquid and a viscoelastic material [23]: in the nonadiabatic regime, the electronic system behaves fluidlike and internal friction leads to dissipative effects. The opposing regime is characterized by solidlike elastic behavior as for HPT motion or in the limiting case of infinite frequency. The effects that are crucial in the latter regime are thus mainly incorporated into the exact ground state $v_{xc,0}$. Hence, the adiabatic approximation works well in the elastic regime.

The small perturbation limit also leads to the linear response regime of TDDFT. Here memory effects are known to be crucial for the correct representation of double and multiple excitations [4,8]. Investigating these questions using the adiabatically exact approximation has been the topic of a recent study [52]. Earlier studies [46] have already established a connection between dissipative effects and nonadiabatic corrections to linear response quantities.

Of course the ultimate goal is the development of xc functionals that are applicable both in the adiabatic and nonadiabatic regimes. Currently, there is a lot of progress going on in this direction [23,53–58] with most of these approaches drawing from hydrodynamic concepts. The present work shows that both the QFD approach and the 1D two-electron singlet system as a benchmark case can provide important guidance on this route.

ACKNOWLEDGMENTS

M.T. is grateful for stimulating discussions with Hans Schamel, Wolf-Christian Müller, and Ralf Kaiser. S.K. and M.T. acknowledge support by the Deutsche Forschungsgemeinschaft.

APPENDIX A: CLASSICAL FLUID DYNAMICS

In classical fluid dynamics (cf., e.g., Refs. [49,59]), the flow of a medium is described in terms of the density field $n(\mathbf{r},t)$, the velocity field $\boldsymbol{u}(\mathbf{r},t)$, and the stress tensor $\Pi(\mathbf{r},t)$. The first governing equation is the continuity equation,

$$D_t n = -n\,\boldsymbol{\nabla}\cdot\boldsymbol{u}, \tag{A1}$$

where the material or convective derivative $D_t=\partial_t+\boldsymbol{u}\cdot\boldsymbol{\nabla}$ describes the rate of change following the fluid. An important special case is provided by incompressible flow corresponding to $\boldsymbol{\nabla}\cdot\boldsymbol{u}=0$. In this case the rhs of the continuity equation vanishes and the density is just transported or advected with the flow, i.e., no compression and rarefaction takes place.

To determine the velocity field a second evolution equation is required; the momentum balance

$$mD_t\boldsymbol{u} = \frac{1}{n}\boldsymbol{\nabla}\cdot\Pi - \boldsymbol{\nabla}v_{ext}. \tag{A2}$$

Here, the divergence of the stress tensor Π represents internal forces whereas $\boldsymbol{\nabla}v_{ext}(\mathbf{r},t)$ describes external body forces acting on the fluid. $\Pi_{ij}=-p\delta_{ij}+\sigma_{ij}$ contains the scalar hydrostatic pressure $p(\mathbf{r},t)$, a nonideal contribution, and the viscous shear-stress tensor $\sigma_{ij}(\mathbf{r},t)$. These quantities have to be determined from constitutive equations, which formally close the system of equations. For a classical Newtonian fluid,

$$\sigma_{ij} = \eta\left[\partial_j u_i + \partial_i u_j - \tfrac{2}{3}\delta_{ij}\boldsymbol{\nabla}\cdot\boldsymbol{u}\right] + \zeta\delta_{ij}\boldsymbol{\nabla}\cdot\boldsymbol{u}, \tag{A3}$$

where η and ζ are the shear and the bulk viscosity of the liquid. These material properties and an equation of state for the pressure p are required as further input into the theory. For constant η and ζ Eq. (A2) turns into the famous Navier-Stokes equation.

Obviously σ depends on spatial derivatives of the velocity field and accounts for viscous effects in the fluid. It is set to zero for an inviscid flow for which the Navier-Stokes equation reduces to the Euler equation,

$$mD_t\boldsymbol{u} = -\frac{1}{n}\boldsymbol{\nabla}p - \boldsymbol{\nabla}v_{ext}. \tag{A4}$$

The absence of dissipation in the latter equation is the reason for major differences to the Navier-Stokes equation: flow governed by the Euler equation can build up shocks that would otherwise be attenuated by dissipation. Furthermore, viscous effects are crucial in the context of turbulence, which is the prevalent flow state of most classical fluids. These phenomena are all related to the intrinsic nonlinearity of both the Euler and Navier-Stokes equations, which is provided by the term $\boldsymbol{u}\cdot\boldsymbol{\nabla}\boldsymbol{u}$ in the convective derivative.

We conclude this short review with the 1D version of the Navier-Stokes equation for the z component u,

$$mD_t u = \frac{1}{n}\partial_z \tilde{p} - \partial_z v_{\text{ext}}, \tag{A5}$$

where the stress-tensor Π has taken the form of a generalized pressure $\tilde{p}$. Naturally the latter still contains the hydrostatic pressure p and dynamical contributions from σ_{zz}.

APPENDIX B: QUANTUM FLUID DYNAMICS

While the classical hydrodynamic equations just represent a continuum approximation to the classical mechanics of point particles, many-body quantum mechanics based on the continuous wave function can be exactly transformed into quantum fluid dynamics (QFD) [28].

The derivation for a single-particle wave function $\varphi(\mathbf{r},t)$ [12] starts by inserting $\varphi(\mathbf{r},t)=R(\mathbf{r},t)e^{i\alpha(\mathbf{r},t)}$ with R and α real into

$$i\hbar\partial_t\varphi(\mathbf{r},t) = \left(-\frac{\hbar^2}{2m}\nabla^2 + v_{\text{ext}}(\mathbf{r},t)\right)\varphi(\mathbf{r},t). \tag{B1}$$

Separating real and imaginary parts of the equation, realizing that $R^2=|\varphi|^2=n$, and defining $\boldsymbol{u}=\frac{\hbar}{m}\boldsymbol{\nabla}\alpha$ one arrives at

$$D_t n = -n\,\boldsymbol{\nabla}\cdot\boldsymbol{u} \tag{B2}$$

and

$$mD_t u_j = -\frac{1}{n}\partial_i P_{ij} - \partial_j v_{\text{ext}}, \tag{B3}$$

where

$$P_{ij} = \frac{\hbar^2}{4m}\left(\frac{(\partial_i n)(\partial_j n)}{n} - \delta_{ij}\nabla^2 n\right) \tag{B4}$$

is the quantum stress tensor [14,24,28]. The obtained equations show a strong analogy to the continuity and Navier-Stokes equations for classical fluids as presented before.

The QFD equations for the time-dependent two-electron singlet KS system can be derived in the same way using $R^2=|\varphi|^2=n/2$ and v_s instead of v_{ext} or by evaluating the general many-particle form of the noninteracting stress tensor P_{sij} [24–26] for the time-dependent singlet KS wave function. After all factors of 2 have canceled out, we are left with

$$D_t n = -n\,\boldsymbol{\nabla}\cdot\boldsymbol{u}_s \tag{B5}$$

and

$$mD_t u_{sj} = -\frac{1}{n}\partial_i P_{sij} - \partial_j v_s, \tag{B6}$$

where P_{sij} is given by Eq. (B4). Consequently the only difference to the one particle case is that the effective potential v_s still contains two density-dependent contributions v_{hx} and v_c. The most appropriate way to deal with v_{hx} is via a separate Poisson equation,

$$\Delta v_{\text{hx}} = -2\pi e^2 n, \tag{B7}$$

as in the theory of conducting fluids [60]. On the other hand the unknown v_c is clearly related to internal forces within the system. In analogy with Eq. (A2) it thus makes sense to define the correlation contribution to the stress tensor according to

$$\boldsymbol{\nabla} p_c = n\,\boldsymbol{\nabla} v_c \tag{B8}$$

and group it together with P_{sij} so that [29]

$$mD_t u_{sj} = -\frac{1}{n}\partial_i(P_{sij} + \delta_{ij}p_c) - \partial_j(v_{\text{hx}} + v_{\text{ext}}). \tag{B9}$$

It is also interesting to note that the QFD point of view opens up connections to other fields of physics. The Madelung fluid concept [12] for instance is also employed in the study of solitary waves and the nonlinear Schrödinger equation [43].

APPENDIX C: BEYOND THE 1D TWO-ELECTRON SYSTEM

The basic structure of the QFD equations is not modified for systems of more than two electrons in three dimensions. Thus the adiabatic approximation can still be interpreted as neglecting xc contributions that depend on gradients of the velocity field.

We have seen that in 1D velocity gradients can occur only for compressive flow, which leads to dissipation of classical kinetic energy and can be detected by the proposed criterion. In three dimensions shear flow is another possible source of dissipation through internal friction. Quite appropriately $T_{s,0}$ is governed by

$$\dot{T}_{s,0}(t) = -\int (\partial_j u_{si}) P_{s,0ji} d^3 r, \tag{C1}$$

which means that it is not only sensitive to compression, where $\boldsymbol{\nabla}\cdot\boldsymbol{u}_s \neq 0$ $(i=j)$, but also to shear velocity gradients $(i\neq j)$ multiplied by off-diagonal elements of $P_{s,0ji}$. As the time-scale argument based on the xc kernel does also remain valid the criterion can thus be formulated as in one dimension.

Of course the presence of more than two particles means that different single-particle currents can contribute to the total current. Whether this will lead to additional nonadiabatic effects that are not detected by the proposed criterion cannot be established at present. However the violation of the breakdown criterion should still provide a definitive warning signal for an ongoing TDKS calculation.

[1] *Time-Dependent Density Functional Theory*, edited by M. Marques, C. Ullrich, F. Nogueira, A. Rubio, K. Burke, and E. Gross (Springer, Berlin, 2006).
[2] P. B. Corkum and F. Krausz, Nat. Phys. **3**, 381 (2007).
[3] M. Lein, E. K. U. Gross, and J. P. Perdew, Phys. Rev. B **61**, 13431 (2000).
[4] N. T. Maitra, F. Zhang, R. J. Cave, and K. Burke, J. Chem. Phys. **120**, 5932 (2004).
[5] P. Hessler, N. T. Maitra, and K. Burke, J. Chem. Phys. **117**, 72 (2002).
[6] H. O. Wijewardane and C. A. Ullrich, Phys. Rev. Lett. **95**, 086401 (2005).
[7] C. A. Ullrich and I. V. Tokatly, Phys. Rev. B **73**, 235102 (2006).
[8] C. A. Ullrich, J. Chem. Phys. **125**, 234108 (2006).
[9] H. O. Wijewardane and C. A. Ullrich, Phys. Rev. Lett. **100**, 056404 (2008).
[10] I. D'Amico and G. Vignale, Phys. Rev. B **59**, 7876 (1999).
[11] M. Thiele, E. K. U. Gross, and S. Kümmel, Phys. Rev. Lett. **100**, 153004 (2008).
[12] E. Madelung, Z. Phys. **40**, 322 (1926).
[13] K.-K. Kan and J. J. Griffin, Phys. Rev. C **15**, 1126 (1977).
[14] S. K. Ghosh and B. M. Deb, Phys. Rep. **92**, 1 (1982).
[15] B. M. Deb and S. K. Ghosh, J. Chem. Phys. **77**, 342 (1982).
[16] E. Runge and E. K. U. Gross, Phys. Rev. Lett. **52**, 997 (1984).
[17] E. K. U. Gross, J. F. Dobson, and M. Petersilka, in *Density Functional Theory*, edited by R. F. Nalewajski (Springer, Berlin, 1996), pp. 81–172.
[18] R. van Leeuwen, Phys. Rev. Lett. **82**, 3863 (1999).
[19] S. Kümmel, K. Andrae, and P.-G. Reinhard, Appl. Phys. B: Lasers Opt. **73**, 293 (2001).
[20] K. Capelle, J. Chem. Phys. **119**, 1285 (2003).
[21] J. F. Dobson, Phys. Rev. Lett. **73**, 2244 (1994).
[22] G. Vignale and W. Kohn, Phys. Rev. Lett. **77**, 2037 (1996).
[23] G. Vignale, C. A. Ullrich, and S. Conti, Phys. Rev. Lett. **79**, 4878 (1997).
[24] I. V. Tokatly, Phys. Rev. B **71**, 165104 (2005).
[25] I. V. Tokatly, Phys. Rev. B **71**, 165105 (2005).
[26] I. V. Tokatly, in *Time-Dependent Density Functional Theory*, edited by M. Marques, C. Ullrich, F. Nogueira, A. Rubio, K. Burke, and E. Gross (Springer, Berlin, 2006), pp. 123–136.
[27] R. D'Agosta and M. Di Ventra, J. Phys.: Condens. Matter **18**, 11059 (2006).
[28] R. D'Agosta and M. Di Ventra, J. Phys.: Condens. Matter **20**, 374102 (2008).
[29] J. Tao, G. Vignale, and I. V. Tokatly, Phys. Rev. Lett. **100**, 206405 (2008).
[30] D. Bauer, Phys. Rev. A **56**, 3028 (1997).
[31] D. G. Lappas, A. Sanpera, J. B. Watson, K. Burnett, P. L. Knight, R. Grobe, and J. H. Eberly, J. Phys. B **29**, L619 (1996).
[32] D. G. Lappas and R. van Leeuwen, J. Phys. B **31**, L249 (1998).
[33] W.-C. Liu, J. H. Eberly, S. L. Haan, and R. Grobe, Phys. Rev. Lett. **83**, 520 (1999).
[34] M. Lein, E. K. U. Gross, and V. Engel, Phys. Rev. Lett. **85**, 4707 (2000).
[35] S. L. Haan and R. Grobe, Laser Phys. **8**, 885 (1998).
[36] P. Hohenberg and W. Kohn, Phys. Rev. **136**, B864 (1964).
[37] M. Lein and S. Kümmel, Phys. Rev. Lett. **94**, 143003 (2005).
[38] A. S. de Wijn, S. Kümmel, and M. Lein, J. Comput. Phys. **226**, 89 (2007).
[39] N. T. Maitra, K. Burke, and C. Woodward, Phys. Rev. Lett. **89**, 023002 (2002).
[40] G. Vignale, Phys. Rev. Lett. **74**, 3233 (1995).
[41] This choice of parameters leads to density distributions that can be well represented on the used numerical grid.
[42] N. Maitra, K. Burke, H. Appel, E. Gross, and R. van Leeuwen, in *Ten Topical Questions in Time-Dependent Density Functional Theory*, edited by K. D. Sen (World Scientific, Singapore, 2002), pp. 1186–1225.
[43] R. Fedele and H. Schamel, Eur. Phys. J. B **27**, 313 (2002).
[44] G. Giuliani and G. Vignale, *Quantum Theory of the Electron Liquid* (Cambridge University Press, Cambridge, 2005).
[45] C. A. Ullrich and G. Vignale, Phys. Rev. B **58**, 15756 (1998).
[46] C. A. Ullrich and K. Burke, J. Chem. Phys. **121**, 28 (2004).
[47] F. Calvayrac, P. G. Reinhard, E. Suraud, and C. A. Ullrich, Phys. Rep. **337**, 493 (2000).
[48] R. D'Agosta and G. Vignale, Phys. Rev. Lett. **96**, 016405 (2006).
[49] D. Acheson, *Elementary Fluid Dynamics* (Clarendon, Oxford, 1990).
[50] It appears highly unlikely that the frequency dependence of the inverse interacting and noninteracting response functions directly cancels at the lowest transition frequency.
[51] R. Baer, e-print arXiv:0808.3848, J. Mol. Struct.: THEOCHEM (in press).
[52] M. Thiele and S. Kümmel, Phys. Chem. Chem. Phys. (in press).
[53] Y. Kurzweil and R. Baer, Phys. Rev. B **72**, 035106 (2005).
[54] Y. Kurzweil and R. Baer, Phys. Rev. B **73**, 075413 (2006).
[55] E. Orestes, K. Capelle, A. B. F. da Silva, and C. A. Ullrich, J. Chem. Phys. **127**, 124101 (2007).
[56] J. F. Dobson, M. J. Bünner, and E. K. U. Gross, Phys. Rev. Lett. **79**, 1905 (1997).
[57] C. A. Ullrich, U. J. Gossmann, and E. K. U. Gross, Phys. Rev. Lett. **74**, 872 (1995).
[58] I. V. Tokatly, Phys. Rev. B **75**, 125105 (2007).
[59] G. K. Batchelor, *An Introduction to Fluid Dynamics* (Cambridge University Press, Cambridge, 1967).
[60] J. Goedbloed and S. Poedts, *Principles of Magnetohydrodynamics* (Cambridge University Press, Cambridge, 2004).